FEBS Letters 482 (2000) 180–184 FEBS 24136

Interaction of different oligomeric states of hexameric DNA-helicase RepA with single-stranded DNA studied by analytical ultracentrifugation

Hai Xu[a], Joachim Frank[b,*], Josef F. Holzwarth[b], Wolfram Saenger[a], Joachim Behlke[c]

[a] *Institut für Kristallographie, Freie Universität Berlin, Takustr. 6, D-14195 Berlin, Germany*
[b] *Fritz-Haber-Institut der Max-Planck-Gesellschaft, Faradayweg 4–6, D-14195 Berlin, Germany*
[c] *Max-Delbrück-Centrum für Molekulare Medizin, Robert-Rössle-Str. 10, D-13122 Berlin, Germany*

Received 29 June 2000; revised 29 August 2000; accepted 30 August 2000

Edited by Ned Mantei

Abstract Analytical ultracentrifugation was used to determine the molecular mass, *M*, of hexameric DNA-helicase RepA at pH 5.8 and 7.6. At pH 7.6, a molecular mass of 179.5 ± 2.6 kDa was found, consistent with the known hexameric state of RepA, $(RepA)_6$. At pH 5.8, $(RepA)_6$ associates to form a dimer with a molecular mass of 366.2 ± 4.1 kDa. Analytical ultracentrifugation was also applied to characterize the interaction of single-stranded DNA (ssDNA) with the two different oligomeric states of $(RepA)_6$ at pH 5.8 and 7.6. The dissociation constants, K_d, for the equilibrium binding of $(dA)_{30}$ to the $(RepA)_6$ dimer at pH 5.8 and to $(RepA)_6$ at pH 7.6 were determined at 10°C in the presence of 0.5 mM ATPγS, 10 mM $MgCl_2$ and 60 mM NaCl as $K_{d5.8} = 0.94 \pm 0.13$ μM at pH 5.8 and $K_{d7.6} = 25.4 \pm 6.4$ μM at pH 7.6. The stoichiometries, *n*, for the two complexes $(dA)_{30}$/$(RepA)_6$ dimer and $(dA)_{30}$/$(RepA)_6$ at pH 5.8 and 7.6 were calculated from the corresponding binding curves. At pH 5.8 one $(dA)_{30}$ molecule was bound per $(RepA)_6$ dimer, while at pH 7.6 one $(dA)_{30}$ molecule was bound to one $(RepA)_6$. Binding curves were compatible with a single ssDNA binding site present on the $(RepA)_6$ dimer and on $(RepA)_6$, respectively, with no indication of cooperativity. $(RepA)_6$ tends to form larger aggregates under acidic conditions (pH < 6.0) which are optimal for ssDNA binding. In contrast, at pH 5.8 in the presence of 60 mM NaCl, only the $(RepA)_6$ dimer was observed both in the absence and presence of $(dA)_{30}$.

Key words: RepA; Single-stranded DNA; Equilibrium binding; Stoichiometry; Analytical ultracentrifugation

1. Introduction

Helicases are a family of motor proteins utilizing nucleoside 5′-triphosphate hydrolysis for the unwinding of nucleic acid double helices [1]. They are essential for replication, transcription, recombination and repair of double-stranded DNA (dsDNA). For the binding of helicase and initiation of unwinding of dsDNA, single-stranded regions of DNA or loader proteins are required. The unwinding reaction is strictly processive in 5′ to 3′ or 3′ to 5′ direction depending on the helicase under study, with the former being encountered more frequently. Despite extensive biochemical studies on helicases, the mechanism of the unwinding reaction is not yet understood in detail.

Helicases are composed of two or six identical subunits. DnaB-helicase from *Escherichia coli* exists as a ring-shaped hexamer over a large concentration range. Depending on the pH and cofactors present, DnaB-helicase can form a triangle-shaped oligomer built by a trimer of dimers [2]. Bacteriophage T7 gene 4 helicase and plasmid RSF1010 encoded hexameric RepA helicase ($(RepA)_6$) are also ring-shaped hexamers [3,4]. These helicases have in common a central channel through which single-stranded DNA (ssDNA) is assumed to pass.

$(RepA)_6$ is one of the smallest known DNA-helicases with a molecular mass of 6×29 896 kDa [4,5]. In contrast to other multimeric helicases which require Mg^{2+}, ATP or ssDNA to assemble into multimeric forms, the hexameric structure of $(RepA)_6$ is stable even in the absence of any cofactor. The optimum of the helicase activity of $(RepA)_6$ is around pH 5.5–6.0, a property that is shared only by DNA-helicases from *Saccharomyces cerevisiae* [6], whereas all other helicases are optimally active around neutral pH. $(RepA)_6$ assembles into tubular aggregates below pH 6.0. It could be crystallized at that pH [7], and the three-dimensional structure determined by X-ray diffraction methods was refined to 2.4 Å resolution (Niedenzu et al., submitted for publication). $(RepA)_6$ is pot-shaped with a 110 Å outer diameter and 60 Å height, and contains a central hole with 17 Å diameter. The six monomers in $(RepA)_6$ possess the same conformation, and model building studies suggest that ATP is wedged into clefts between monomers, with the triphosphate moieties located in Walker A motifs typical of ATP hydrolyzing enzymes (Niedenzu et al., submitted for publication). In the crystals, $(RepA)_6$ are orientated back-to-back to form dimers of hexamers stabilized by direct protein–protein contacts. The dimers are stacked like coins in a roll, giving rise to cylinders reminiscent of the tubular structures mentioned above, that form at pH < 6.0. The position of ATP between adjacent monomers in $(RepA)_6$ could explain the cooperativity of binding of ATP and of the non-hydrolyzable analog adenosine-5′-*O*-(3-thiotriphosphate) (ATPγS) to $(RepA)_6$, with Hill coefficients around 2.0 (Xu et al., submitted for publication).

Because ssDNA stimulates the hydrolysis of ATP, it is of interest to further investigate the binding of ssDNA to $(RepA)_6$, which is the topic of this study. Since one ssDNA is assumed to pass through the central channel of ring-shaped helicases during the unwinding reaction while the second ssDNA strand moves along the outsite of the helicase mole-

*Corresponding author. Fax: (49)-30-8413 3155.
E-mail: frank_j@fhi-berlin.mpg.de

Abbreviations: ssDNA, single-stranded DNA; dsDNA, double-stranded DNA; ATPγS, adenosine-5′-*O*-(3-thiotriphosphate); MES, 2-(*N*-morpholino)ethane sulfonic acid; $(RepA)_6$, RepA hexamer

PII: S0014-5793(00)02026-3

cule, the question arises how many binding sites for ssDNA molecules are present on hexameric helicases. To answer this question, we measured the dissociation constants, K_d, and the stoichiometries, n, for the binding of $(dA)_{30}$ to purified $(RepA)_6$ at optimum and minimum helicase activity at pH 5.8 and 7.6 [4,5], respectively, by using analytical ultracentrifugation.

2. Materials and methods

All salts and buffer components were purchased from Merck (Darmstadt, Germany). The $(dA)_{30}$ oligodeoxynucleotide was purchased from TIB MOLBIOL (Berlin, Germany). DNA-helicase $(RepA)_6$ was purified from *E. coli* as described by Röleke et al. [7]. For investigating the interaction of $(dA)_{30}$ with $(RepA)_6$, two different buffers, A and B, were used. They consist of (A) 40 mM 2-(*N*-morpholino)ethane sulfonic acid (MES)–NaOH, 10 mM $MgCl_2$, 60 mM NaCl, pH 5.8, and (B) 40 mM Tris–HCl, 10 mM $MgCl_2$, 60 mM NaCl, pH 7.6. Buffer B was also used with no NaCl added as indicated.

2.1. Analytical ultracentrifugation

2.1.1. Theoretical considerations

2.1.1.1. Molecular mass determination. In order to study $(RepA)_6$ under different pH and salt conditions, ultracentrifugation experiments were performed using an XL-A analytical ultracentrifuge (Beckman, Palo Alto, CA, USA) equipped with absorbance optics. For determination of the molecular mass, M, of $(RepA)_6$, the sedimentation equilibrium technique was applied which allows the determination of M directly according to:

$$c_{(r)} = c_0 e^{MF} \tag{1}$$

with

$$F = \frac{(1-\rho\bar{v})\omega^2(r^2-r_0^2)}{2RT} \tag{2}$$

where ρ is the solvent density, $\bar{v}$ is the partial specific volume of $(RepA)_6$, ω is the angular velocity, R is the gas constant, T is the absolute temperature, $c_{(r)}$ is the radial concentration and c_0 is the corresponding value at the meniscus position.

In addition to the molecular mass obtained, the determined parameters allow calculation of the volume, V, of the solute:

$$V = \frac{M\bar{v}}{N_A} \tag{3}$$

with N_A as Avogadro's number.

Assuming that a protein molecule has a spherical shape, the radius, r, of the unhydrated protein is given by:

$$r = \sqrt[3]{\frac{3V}{4\pi}} \tag{4}$$

In aqueous solution, the radius is larger by about 0.3 nm (water shell).

2.1.1.2. Complex formation between (RepA)$_6$ and (dA)$_{30}$. Complex formation between different macromolecules can be easily detected from mass determinations when the associates are formed with high affinity ($K_a > 10^8$ M^{-1}). Because complex formation is often weak, it is necessary to estimate the association constants of an interacting system by fitting the sum of exponential functions, given in Eq. 5, to the experimentally obtained radial scanning curves [8]:

$$A_r = \varepsilon_R c_R e^{BM_R F} + \varepsilon_L c_L e^{M_L F} + c_R \sum_{j=1}^{n} (\varepsilon_R + j\varepsilon_L) c_L^j K_j e^{(BM_R + jM_L)F} \tag{5}$$

where ε_R, ε_L, c_R and c_L are the extinction coefficients and concentrations of the free protein molecule (R = $(RepA)_6$) or the free ligand concentration (L = $(dA)_{30}$) at the radial position r_0, respectively. B is the difference in buoyancy between R and L, j is the number of possible binding steps, and K_j is the binding constant corresponding to one binding step. To obtain more precise data for the estimated parameters, we have to reduce the number of variables describing the binding reaction by (i) separate determination of molecular masses, (ii) using a statistical binding model for equal binding sites [9], and (iii) taking the mass conservation into account. In each experiment, three absorbance profiles were measured at three different wavelengths. This allowed determination of the total concentration in an arbitrary sector by numerical integration. According to a statistical model, K_j is given by:

$$K_j = (1/n^j)\binom{n}{j} K_1^j \tag{6}$$

where K_1 is the binding constant for the first step. If one substitutes $(1/n^j)\binom{n}{j}$ with G_j, and $1/K_1$ with K_d or $c_L K_1 = x$, Eq. 5 can be written as [10]:

$$A_r = \varepsilon_R c_R e^{BM_R F} + \varepsilon_L K_d x e^{M_L F} + c_R \sum_{j=1}^{n} (\varepsilon_R + j\varepsilon_L) G_j x^j e^{(BM_R + jM_L)F} \tag{7}$$

For the total concentrations c_{Rt} and c_{Lt}, the integration of the model function results in:

$$c_{Rt}(r_b - r_m) = c_R \left[\int_{r_m}^{r_b} e^{BM_R F} dr + \sum_{j=1}^{n} x^j G(j) \int_{r_m}^{r_0} e^{(BM_R + jM_L)F} dr \right] \tag{8}$$

$$c_{Lt}(r_b - r_m) = \left[K_d x \int_{r_m}^{r_b} e^{M_L F} dr + c_R \sum_{j=1}^{n} j x^j G(j) \int_{r_m}^{r_0} e^{(BM_R + jM_L)F} dr \right] \tag{9}$$

with r_b and r_m being the radius position at the bottom of the cell and the meniscus, respectively. The substitution of c_R and K_d by functions of Eqs. 8 and 9 allows reduction of the number of estimated parameters to only c_L. Three of the absorbance profiles (Eq. 8 or 9 represents such a profile only for one wavelength) were simultaneously fitted (global) by non-linear regression using the program 'Polymole' which was successfully applied earlier in the analysis of other complexes [8,11–14]. The optimal fit to the radial distribution curves allowed estimation of the dissociation constant of the complex.

2.1.2. Experimental setup. For determination of the molecular mass, M, the sedimentation equilibrium data were analyzed by means of externally loaded six-channel centerpieces of 12 mm optical path length filled with 70 μl of solution in the corresponding compartment. This cell type allows the analysis of three solvent/solution pairs. The protein concentration was adjusted to 0.16–0.48 mg/ml throughout. The sedimentation equilibrium was reached after 2 h overspeed at 14 000 rpm, followed by an equilibrium speed of 10 000 rpm at 10°C for about 30 h. The radial absorbancies of each compartment were recorded at three different wavelengths, 280, 285 and 290 nm at pH 7.6 and, 275, 280 and 285 nm at pH 5.8. The molecular mass, M, determinations were done by simultaneously fitting the three radial absorbance distribution curves according to Eqs. 1 and 2 applying a partial specific volume, $\bar{v} = 0.74$ g cm^{-3} which was calculated from the known amino acid sequence of $(RepA)_6$ and the density increment.

To study complex formation between $(RepA)_6$ and $(dA)_{30}$, radial distribution curves were measured by means of externally loaded six-channel centerpieces of 12 mm optical path length filled with 70 μl of solution in the corresponding compartment. The radial absorbancies of each compartment were measured at three different wavelengths, 280, 285 and 290 nm at pH 5.8 and, 275, 280 and 285 nm at pH 7.6 after 2 h overspeed at 14 000 rpm, followed by an equilibrium speed of 10 000 rpm at 10°C for about 30 h. The protein and oligonucleotide concentrations were adjusted to 0.46 μM $(RepA)_6$ dimer and 0–1.84 μM $(dA)_{30}$ at pH 5.8, respectively. At pH 7.6, protein and oligodeoxynucleotide concentrations of 1.87 μM $(RepA)_6$ and 0–6.5 μM $(dA)_{30}$ were used, respectively. The dissociation constants of the complex between $(RepA)_6$ and $(dA)_{30}$ and the concentrations of free $(RepA)_6$, free $(dA)_{30}$ and their complexes were determined at pH 5.8 and 7.6 by fitting the three radial distribution curves to Eqs. 7–9. To calculate the stoichiometries for the binding reaction, the concentration of the complex was determined for different molar ratios, $(dA)_{30}/(RepA)_6$ dimer and $(dA)_{30}/(RepA)_6$, at pH 5.8 and 7.6, respectively. The concentration of the complex per $(RepA)_6$ dimer was plotted as a function of the molar ratio $(dA)_{30}/(RepA)_6$ dimer at pH 5.8.

At pH 7.6, the concentration of the complex per $(RepA)_6$ was plotted as a function of the molar ratio $(dA)_{30}/(RepA)_6$.

3. Results

Fig. 1A,B shows typical radial distribution functions for $(RepA)_6$ at pH 5.8 and 7.6, respectively. From the fit of Eqs. 1 and 2 to the radial distribution functions, the molecular masses, M, of $(RepA)_6$ were determined to be 366.2 ± 4.1 kDa at pH 5.8 (buffer A) and 179.5 ± 2.6 kDa at pH 7.6 (buffer B). In both cases 60 mM NaCl was included in the applied buffer systems. At pH 7.6, the molecular mass of $(RepA)_6$ was measured in the absence of NaCl using buffer B (data not shown) and determined as 188.6 ± 2.8 kDa. To avoid higher aggregation at pH 5.8, the molecular mass of $(RepA)_6$ was measured in the presence of 60 mM NaCl where no aggregation of $(RepA)_6$ was observed up to protein concentrations of 0.48 mg/ml. For all concentrations studied (0.16–0.48 mg/ml) at pH 5.8 the molecular mass of 366.2 ± 4.1 kDa corresponds

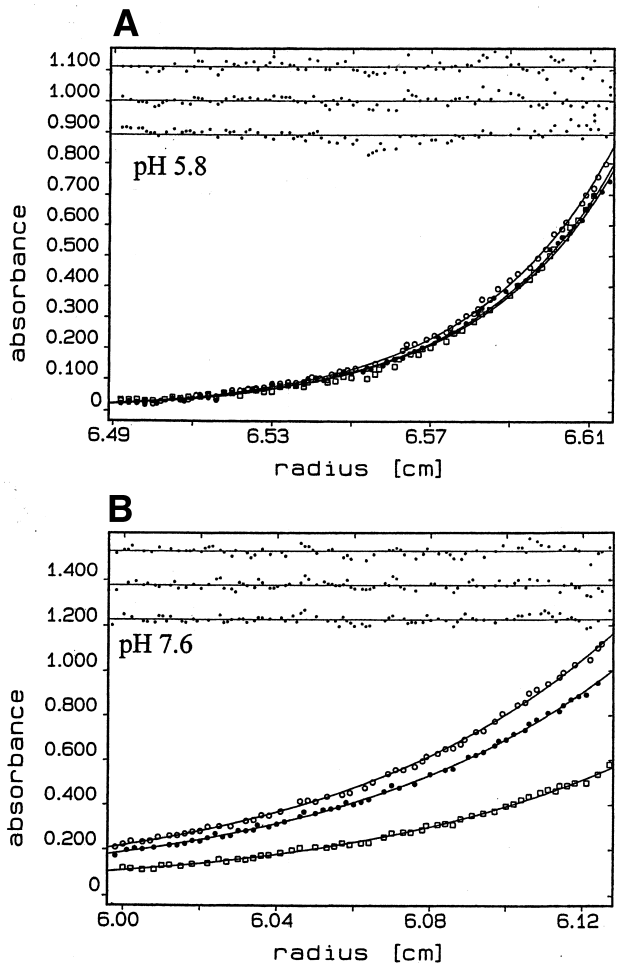

Fig. 1. A: Sedimentation equilibrium runs monitored at 275 (●), 280 (○) and 285 (□) nm, pH 5.8. $(RepA)_6$ concentration was 2.67 μM in 40 mM MES–NaOH, 10 mM $MgCl_2$, and 60 mM NaCl at pH 5.8. From fits of Eqs. 1 and 2, a molecular mass of 357.9 ± 2.9 kDa was determined for a dimer of $(RepA)_6$ at pH 5.8. B: Sedimentation equilibrium runs monitored at 280 (○), 285 (●) and 290 (□) nm. $(RepA)_6$ concentration was 2.67 μM in 40 mM Tris–HCl, 10 mM $MgCl_2$ and 60 mM NaCl at pH 7.6. From fits of Eqs. 1 and 2 a molecular mass of 179.5 ± 2.6 kDa was determined for $(RepA)_6$ at pH 7.6.

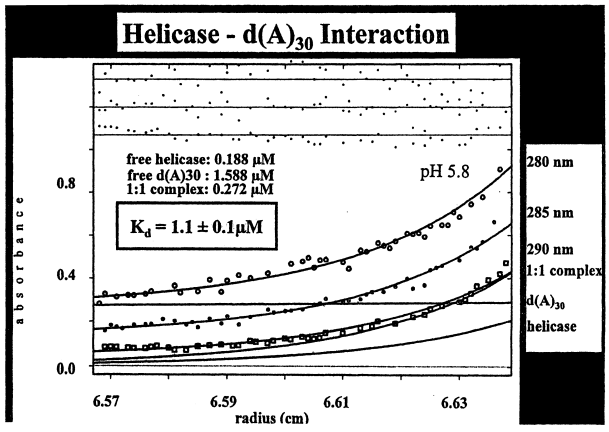

Fig. 2. Radial distribution functions monitored at 280 (○), 285 (●) and 290 (□) nm. $(RepA)_6$ dimer concentration was 0.46 μM in 40 mM MES–NaOH, 10 mM $MgCl_2$, and 60 mM NaCl, pH 5.8; $[(dA)_{30}] = 1.86$ μM. From fits of Eqs. 7, 8 and 9 to the radial distribution functions, a dissociation constant, K_d, for the $(RepA)_6$ dimer of 1.1 ± 0.1 μM was determined.

to the dimer of $(RepA)_6$. The equilibrium between $(RepA)_6$ and $(RepA)_6$ dimer is shifted at pH 5.8 to the dimer and no $(RepA)_6$ (molecular mass = 180 kDa) could be detected.

Fig. 2 shows the radial distribution curves of the complexes between $(dA)_{30}$ and $(RepA)_6$ dimer at pH 5.8. Fits of Eqs. 7–9 to the radial distribution curves allowed determination of the dissociation constants, K_d, for the binding of $(dA)_{30}$ to $(RepA)_6$ dimer at pH 5.8 and to $(RepA)_6$ at pH 7.6. Fig. 3A,B shows the binding curves for the titration of $(RepA)_6$ dimer at pH 5.8 and of $(RepA)_6$ at pH 7.6 with increasing concentrations of $(dA)_{30}$ in the presence of 0.5 mM ATPγS. For the determination of dissociation constants, Eqs. 7–9 were fitted to the radial distribution functions yielding also the concentrations of the complexes, free $(RepA)_6$ and free $(dA)_{30}$. The concentration of the complex $((dA)_{30}/(RepA)_6)$ per $(RepA)_6$ dimer $((RepA)_6)$ was plotted against the molar ratio $(dA)_{30}/(RepA)_6$ dimer $((RepA)_6)$ at pH 5.8 (pH 7.6) to determine the stoichiometry of the binding reaction. The data are consistent with the binding of ssDNA to a single binding site present on $(RepA)_6$ (pH 7.6) or the $(RepA)_6$ dimer (pH 5.8). For the dissociation constant K_d, of the complex between $(RepA)_6$ dimer and $(dA)_{30}$, a value of 0.94 ± 0.13 μM at pH 5.8 was measured in the presence of 0.5 mM ATPγS, 10 mM $MgCl_2$ and 60 mM NaCl at 10°C. For the complex between $(RepA)_6$ and $(dA)_{30}$, a value for K_d of 25.4 ± 6.4 μM at pH 7.6 was obtained at 10°C with 0.5 mM ATPγS, 10 mM $MgCl_2$ and 60 mM NaCl.

4. Discussion

In solution, $(RepA)_6$ exists as a homohexamer of 180 kDa [7]. This finding was confirmed at pH 7.6 by analytical ultracentrifugation experiments. In contrast to the results at pH 7.6, the $(RepA)_6$ dimer was found at pH 5.8 in the absence of a stable ATP analogue. It was shown previously that a number of hexameric helicases including rho and bacteriophage T4 gp41 form dimers of hexamers in solution [15]. The increase in mass of $(RepA)_6$ upon binding of $(dA)_{30}$ is significant enough to enable the determination of K_d by analytical ultracentrifugation experiments. Based on these studies, a common mechanism for complex formation in solution can be derived.

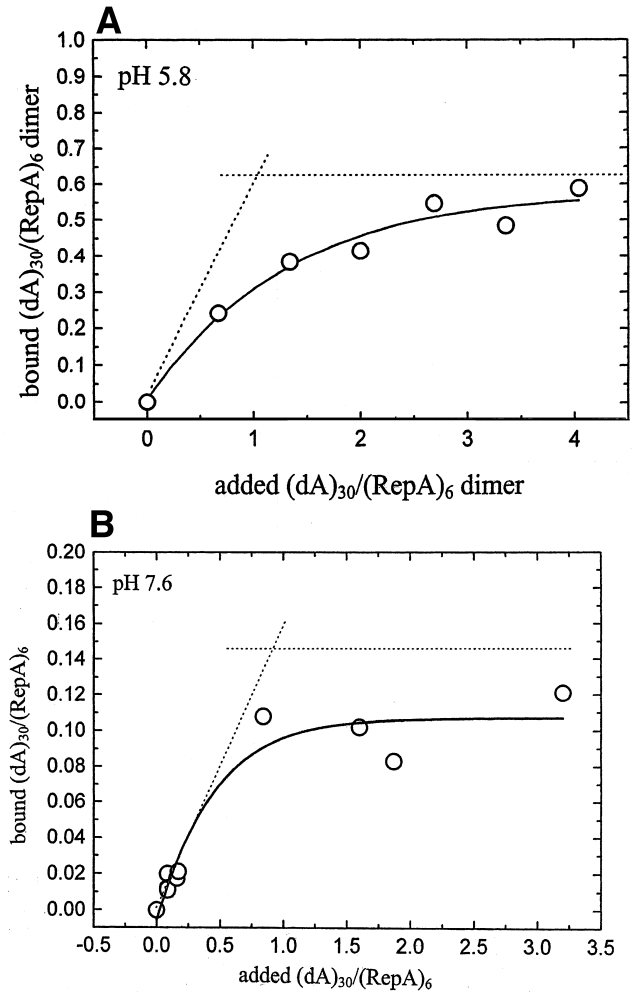

Fig. 3. A: Binding curve for $(RepA)_6$ dimer and $(dA)_{30}$ measured at pH 5.8. The stoichiometry (1:1) of the binding reaction was determined by plotting the concentration of the complex divided by the $(RepA)_6$ dimer concentration (0.46 μM) as a function of the molar ratio $(dA)_{30}/(RepA)_6$ dimer ($K_d = 0.94 \pm 0.13$ μM). B: Binding curve for $(RepA)_6$ and $(dA)_{30}$ measured at pH 7.6. The stoichiometry (1:1) of the binding reaction was determined by plotting the concentration of the complex divided by the $(RepA)_6$ concentration (1.87 μM) as a function of the molar ratio $(dA)_{30}/(RepA)_6$ ($K_d = 25.4 \pm 6.4$ μM).

As is evident from Fig. 3A,B, the fraction of $(dA)_{30}$ bound to $(RepA)_6$ showed a dependence on the $(dA)_{30}$ concentration typical for binding of ssDNA to a single site present on $(RepA)_6$ (pH 7.6) and on $(RepA)_6$ dimer (pH 5.8). A cooperative binding of ssDNA to $(RepA)_6$ as reported for other helicases [16,17] was not observed in the analytical ultracentrifugation experiments reported here as the curves in Fig. 3A,B are not sigmoidal. These experiments showed that $(RepA)_6$ occurs as a dimer at pH 5.8 (i.e. composed of two hexameric $(RepA)_6$ molecules). The stoichiometry, n, and the dissociation constant, K_d, for the $(dA)_{30}/(RepA)_6$ dimer complex at pH 5.8 were determined to be 1:1 (one $(dA)_{30}$ molecule per $(RepA)_6$ dimer) with a value of 0.94 μM. These findings are in close agreement with our recent fluorescence correlation spectroscopy and photon correlation spectroscopy measurements (Xu et al., submitted for publication). At pH 5.8 and 25°C, we determined a dissociation constant, K_d, of 1.1 ± 0.1 μM for the binding of $(dA)_{30}$ to $(RepA)_6$ dimer in the presence of 0.5 mM ATPγS, 10 mM $MgCl_2$ with no added NaCl. Therefore, NaCl up to 60 mM concentration does not influence ssDNA binding to the $(RepA)_6$ dimer.

Since $(RepA)_6$ unwinds any sequence of dsDNA, its binding affinity to ssDNA should be low in comparison to sequence specific proteins; this is in agreement with the present studies. At neutral pH, the affinity of $(RepA)_6$ for ssDNA is so low that it is difficult to measure binding curves.

In the presence of ATP, the RuvB protein forms a dimer on dsDNA in which two stacked hexameric rings encircle the DNA and are orientated in opposite directions (back-to-back) [18]. In the X-ray structure of $(RepA)_6$ crystallized at pH 5.8, a dimer of two hexameric RepA molecules in back-to-back orientation occupies the asymmetric unit (T. Niedenzu, D. Röleke, G. Bains, E. Scherzinger and W. Saenger, submitted for publication). In the case of the helicases DnaB and T4 gp4 it was demonstrated that ssDNA could bind to the central channel of both molecules [19–21]. It is assumed that during the unwinding reaction only one ssDNA passes through the central channel and the other ssDNA moves along the outsite of the helicase. Jezewska et al. have proposed strong and weak ssDNA binding sites present on helicase DnaB which may be involved in the unwinding reaction [21]. According to this model the 5′ end of ssDNA binds strongly to a subsite within the channel, while the ssDNA near the entry site of duplex DNA is only weakly bound. The 3′ ssDNA leaves helicase DnaB at the outsite during the unwinding reaction. From our experiments, we do not know where the ssDNA binds but we observed only a single ssDNA binding site for each $(RepA)_6$ or each dimer of two $(RepA)_6$ with back-to-back orientation. Therefore we can exclude additional weak binding sites present on $(RepA)_6$ in the concentration range studied.

$(RepA)_6$ shows a narrow pH optimum for the dsDNA unwinding reaction in a remarkably low pH range between pH 5.5 and pH 6.0 [4,5]. ssDNA binding to $(RepA)_6$ is also tighter at pH 5.8 compared with pH 7.6 as reported here. Below pH 6.0, $(RepA)_6$ aggregates to form tubular structures, but individual $(RepA)_6$ or $(RepA)_6$ dimers are still present, as shown by electron micrographs taken at pH 5.6 [7]. The radius of $(RepA)_6$ determined by analytical ultracentrifugation agrees well with the geometric constraints of the overall structure of a $(RepA)_6$ dimer. A single $(RepA)_6$ molecule is best described by a cylinder with a radius of 5.5 nm and a height of 6 nm with a central cavity of 1.7 nm in diameter (T. Niedenzu, D. Röleke, G. Bains, E. Scherzinger and W. Saenger, submitted for publication). If two hexameric RepA molecules are arranged back-to-back as shown by the crystal structure, the overall structure is 11 nm × 12 nm, consistent with an apparent radius of 5 nm calculated according to Eqs. 3 and 4.

Acknowledgements: These studies were supported by the Deutsche Forschungsgemeinschaft, by Fonds der Chemischen Industrie and by an EC-project.

References

[1] Matson, S.W. and Kaiser-Rogers, K.A. (1990) Annu. Rev. Biochem. 59, 289–329.
[2] San Martin, M.C., Stamford, N.P.J., Dammerova, N., Dixon, N.E. and Carazo, J.-M. (1995) J. Struct. Biol. 114, 167–176.
[3] Engelman, E.H., Yu, X., Wild, R., Hingorani, M.M. and Patel, S.S. (1995) Proc. Natl. Acad. Sci. USA 92, 3869–3873.

[4] Scherzinger, E., Ziegelin, G., Bárcena, M., Carazo, J.M., Lurz, R. and Lanka, E. (1997) J. Biol. Chem. 272, 30228–30236.
[5] Scherzinger, E., Haring, V. and Otto, S. (1991) Nucleic Acids Res. 19, 1203–1211.
[6] Sung, P., Higgins, D., Prakash, L. and Prakash, S. (1988) EMBO J. 7, 3263–3269.
[7] Röleke, D., Hoier, H., Bartsch, C., Umbach, P., Scherzinger, E., Lurz, R. and Saenger, W. (1997) Acta Cryst. D53, 213–216.
[8] Behlke, J., Ristau, O. and Marg, A. (1995) Prog. Collid Polym. Sci. 94, 40–45.
[9] Wyman, J. and Gill, S.J. (1990) Binding and Linkage, University Science Books, Mill Valley, CA.
[10] Behlke, J., Ristau, O. and Schönfeld, H.-J. (1997) Biochemistry 36, 5149–5156.
[11] Behlke, J., Ristau, O. and Knespel, A. (1994) Prog. Collid Polym. Sci. 99, 63–68.
[12] Grunau, C., Dettmer, R., Behlke, J. and Bernhardt, R. (1995) Biochem. Biophys. Res. Commun. 210, 1001–1008.
[13] Schade, M., Behlke, J., Löwenhaupt, K., Herbert, A., Rich, A. and Oschkinat, H. (1999) FEBS Lett. 458, 27–31.
[14] Kraft, C., Diehl, A., Lättig, S., Behlke, J., Heinemann, U., Pon, C.L., Gualeizi, H. and Welfle, H. (2000) FEBS Lett. 471, 128–132.
[15] Engelman, E.H. (1996) Structure 4, 759–762.
[16] Jezewska, M.J., Kim, U.-S. and Bujalowski, W. (1996) Biochemistry 35, 2129–2145.
[17] Menetski, J.P. and Kowalczykowski, S.C. (1985) J. Mol. Biol. 181, 281–295.
[18] Stasiak, A., Tsaneva, I.R., West, S.C., Benson, C.J.B., Yu, X. and Engelman, E.H. (1994) Proc. Natl. Acad. Sci. USA 91, 7618–7622.
[19] Yu, X., Hingorani, M.M., Patel, S.S. and Engelman, E.H. (1996) Nat. Struct. Biol. 3, 740–743.
[20] Jezewska, M.J., Rajendran, S., Bujalowska, D. and Bujalowski, W. (1998) J. Biol. Chem. 273, 10515–10529.
[21] Jezewska, M.J., Rajendran, S. and Bujalowski, W. (1998) J. Biol. Chem. 273, 9058–9069.